Estimates of Durability of TMI-2 Core Debris Canisters and Cask Liners

A. B. Johnson, Jr.
A. L. Lund
S. P. Pednekar

April 1994

❖ Battelle

PNL-9457

The contents of this report were printed on recycled paper

ESTIMATES OF DURABILITY OF
TMI-2 CORE DEBRIS CANISTERS
AND CASK LINERS

A. B. Johnson, Jr.
A. L. Lund
S. P. Pednekar

April 1994

MASTER

CONTENTS

FIGURES

TABLES

SUMMARY

Core debris from the Three Mile Island-2 (TMI-2) reactor is currently stored in stainless steel canisters. The need to maintain the integrity of the TMI-2 core debris containers through the period of extended storage and possibly into disposal prompted this assessment. In the assessment, corrosion-induced degradation was estimated for two materials: type 304L stainless steel (SS) canisters that contain the core debris, and type 1020 carbon steel (CS) liners in the concrete casks planned for containing the canisters from 2000 AD until the TMI-2 core debris is placed in a repository. Three environments were considered: air-saturated water (with 2 ppm Cl⁻) at 20°C, and air at 20°C with two relative humidities (RHs), 10 and 40%. Corrosion mechanisms assessed included general corrosion (failure criterion: 50% loss of wall thickness) and localized attack (failure criterion: through-wall pinhole penetration). Estimation of carbon steel corrosion after 50 y also was requested.

Durability of Stainless Steel Canisters

Estimates of stainless canister durability during handling, shipping, and wet storage at TMI-2 and the Idaho National Engineering Laboratory (INEL) over the period 1986 - 2000 AD suggest only ~0.2 mil[a] penetration by general corrosion and nil degradation by localized mechanisms.

The following long-term durability results were obtained for 304L stainless steel in exposures beyond 2000 AD in the environments indicated above:

- pinhole penetration:

    - nil in water
    - nil in air

- 50% wall thickness loss[b]:

    - 4600 y in water
    - 11,500 y in air at 10% and 40% RH

The indicated durability of the stainless steel canisters reflects the high corrosion resistance of type 304L stainless steel under the benign conditions expected to prevail in the concrete casks over the period of extended interim storage. Available data suggest that sensitization at welds will be sufficiently low to preclude intergranular penetrations. Corrosion data at 50°C indicate that pitting and crevice factors are close to 1.0,

---

(a) 1 mil = 0.001 in. = 25.4 μm

(b) The general canister wall thickness is 0.25 in. = 250 mils, but the bottom head thickness is 219 mils, which is used as the basis for calculations.

suggesting that these mechanisms are not likely to proceed more rapidly than uniform corrosion, even if they initiate. Galvanic contacts with carbon steel are expected to cathodically polarize the stainless steel and, therefore, will not accelerate corrosion penetrations.

Data on uniform corrosion of type 304L stainless steel were taken from studies in tuff groundwater at 100°C with 7.5 ppm Cl⁻ under a gamma flux. No attempt was made to extrapolate the corrosion data to the more benign conditions that apply to the TMI-2 canisters because some data suggest that the corrosion may not be temperature dependent below ~150°C. Also, the higher gamma flux in the tuff groundwater tests had minimal influence on corrosion of the 304L material. The estimated times for satisfactory durability of the TMI-2 canisters are conservative, but the degree depends on the currently unclear basis for extrapolation.

One of the requested criteria was 50% strength loss; this was interpreted to be represented by 50% penetration of the wall by uniform corrosion.

Durability of Carbon Steel Cask Liners

The following long-term durability results were obtained for type 1020 carbon steel:

environment	penetration after 50 y	time to through-wall pinhole penetration	time to 50% wall thickness loss[a]
water	50 mils	750 y	375 y
air/10% RH	5 mils	7500 y	3800 y
air/40% RH	10 mils	3800 y	1900 y

Carbon steel is susceptible to pitting corrosion and general corrosion in oxygenated water, but pitting and crevice factors are close to one at lower temperatures, so penetrations are similar to general corrosion. Carbon steel is resistant to stress corrosion cracking under the relatively benign conditions expected for the cask liners. While the SS/CS couple tends to promote corrosion of carbon steel, area factors will be similar, minimizing accelerations of localized corrosion.

(a)   The cask liner wall thickness at the thinnest section (floor) is 0.75 in. = 750 mil.

1.0 INTRODUCTION

The Three Mile Island (TMI-2) accident in 1979 resulted in a severely degraded core that included melted and unmelted fuel assembly materials. The rubble from the pressurized-water reactor (PWR) core was placed in stainless steel canisters and was moved to the Idaho National Engineering Laboratory (INEL) in 1986-1990 (Schmitt et al. 19ʓ3). The canisters are currently stored in a pool at Test Area-North (TAN). The next planned action for management of the canisters is to place them in concrete casks with carbon steel liners,[a] where the canisters are expected to reside until a repository is available for final disposal.

The analysis reported here was conducted to evaluate the integrity of the stainless steel (SS) canisters and carbon steel (CS) cask liners. The analysis includes evaluation of both wet (aqueous) and dry (air) modes of storage. Mechanisms were evaluated that include general wall thinning and localized generation of pinholes from corrosion.

1.1 SCOPE OF THE ASSESSMENT

Two components of the storage system were analyzed: the type 304L SS canisters containing the TMI-2 core debris and the type 1020 carbon steel liners of the concrete casks.

The corrosion evaluations were scoped to address two aspects of degradation: 1) pinhole penetration of the canister wall or carbon steel liner, and 2) decrease in wall thickness to one-half of the original value due to uniform corrosion. Three conditions were defined for this assessment: 1) water at 20°C, saturated with air, 2 ppm Cl⁻, inside the concrete casks; and 2) air at 20°C, with two relative humidity (RH) levels: 10% and 40%. Corrosion of the SS canisters was assessed for outer and inner surfaces. One of the three canister types (Fuel, Figure 1) has double containment. All of the canister interiors will be dried and backfilled with air or will remain flooded with water.

Corrosion mechanisms considered for local attack were: pitting, stress corrosion cracking, galvanic attack, and crevice corrosion. The mechanism considered for wall thinning was general corrosion. Microbially influenced corrosion (MIC) was excluded from the assessment due to hydrogen peroxide dosing of the water in the canisters and observations that suggested that MIC was not active (Schmitt et al. 1993).

1.2 APPROACH TO THE ASSESSMENT

The assessment involved identifying corrosion data that are considered relevant to the conditions expected to exist in the canisters and casks. In some cases, data at the relatively benign conditions specified for the analysis were not available; therefore, accessible data at somewhat more

---

(a)   Other options are also being evaluated.

1

aggressive conditions were utilized, resulting in a realistically conservative analysis.

This assessment faced challenges identical to those for other extended storage studies. The assessment had to either demonstrate thermodynamic stability of the affected materials over the expected storage time frame, or identify kinetic data that would serve as the basis for estimates of corrosion behavior of the storage system materials. For this assessment, thermodynamic considerations dictated that the stainless steel and carbon steel would be subject to corrosion; therefore a kinetic approach was necessary. The assessment requested was to estimate a) times for pinhole penetration of the stainless steel canisters and for loss of one-half of the wall thickness; b) estimates for pinhole and uniform penetration of the carbon steel liner after 50 y; and c) times to throughwall pinhole penetration and loss of one-half of the wall thickness for the carbon steel liner.

The assumption of constant saturated oxygen was imposed to simplify the analysis but, in reality, the cask and canister systems are assumed to be closed. Therefore, there will be a gradual decrease in oxygen in the water and air as reaction with the metals occurs. However, a 1,000 R/hr gamma field inside the canisters will generate radiolytic oxygen over the time frame that the field remains significant. The fuel canisters (Figure 1) have catalyst beds to recombine at least part of the radiolytic hydrogen/oxygen inventory, but the gamma fields will also cause radiolysis on the outer canister surfaces.

Are estimates of SS and CS durability over multimillenia credible? The durability of metals over time frames of centuries or millennia has been studied (Johnson and Francis 1980). Innumerable archaeological artifacts, metal meteorites, and native metal masses have survived for periods that are estimated, in some cases, to be several thousand years in a range of environments, including tombs, soils, sea water, caves, and buildings. While iron-based materials have generally been among the least durable, some iron objects have survived over several centuries and, in selected cases, for several millennia. Of particular interest are cases of iron cannon balls from sunken warships; those exposed to oxygenated sea water were severely degraded, while identical objects that were buried in sea sediments resided in conditions that became anoxic, resulting in minimal degradation. Iron objects in the King Tutankhamen tomb survived for more than three millennia with some rusting in an environment that was largely dry, but included periods of moisture incursions. Estimates of multimillenia durability of carbon steel cask liners in air gains some credibility from survival of the Tutankhamen iron artifacts in air. Analogues for the stainless steels do not exist among the ancient metals, but other high-integrity materials, e.g., copper, have survived for several millennia.

1.3 CHARACTERISTICS OF THE TMI-2 FUEL DEBRIS

The TMI-2 core degraded partially by oxidation of the Zircaloy cladding and partially by melting of metals and the oxide fuel pellets. Consequently, the debris in the canisters has a range of characteristics, depending on where it came from in the core. The debris is stored in three types of canisters,

sorted according to size (Figure 1). In some cases, large sections of fuel assemblies and fuel rods are stored; in other cases, the rubble includes melted chunks and whole or fragmented fuel pellets. Some fragments are in the form of fines which were vacuumed from the reactor pressure vessel; they are collected on diatomaceous earth.

The TMI-2 core was in an early stage of exposure when the accident occurred in 1979. The exposure was 92 effective full power days and the core average burnup was ~3000 MWd/MTU. There were 177 PWR fuel assemblies in the core. The degraded core resided in the reactor pressure vessel until 1986 when canning operations began (Table 1). The last canisters were shipped to INEL in 1990. The fission product inventory was relatively small and much of the leachable species would have gone into the core water. Further removal of the leached species would have occurred when the TMI-2 water was removed from the canisters and replaced with TAN water. From the standpoint of the corrosion analysis it is assumed that fission product species are not a factor.

Section 2 of this report examines thermodynamic aspects of the carbon steel behavior. Materials, designs, and conditions are summarized in Section 3. Section 4 provides an estimate of the degree of degradation of the 304L canisters during shipping and during wet storage at TMI-2 and at INEL. Estimated degradation of stainless steel canisters and carbon steel cask liners is given in Section 5 for wet and dry storage modes. Section 5 also includes calculational bases and rationales for the matrix of twelve material and environmental conditions. A concise discussion of the durability assessment appears in Section 6.
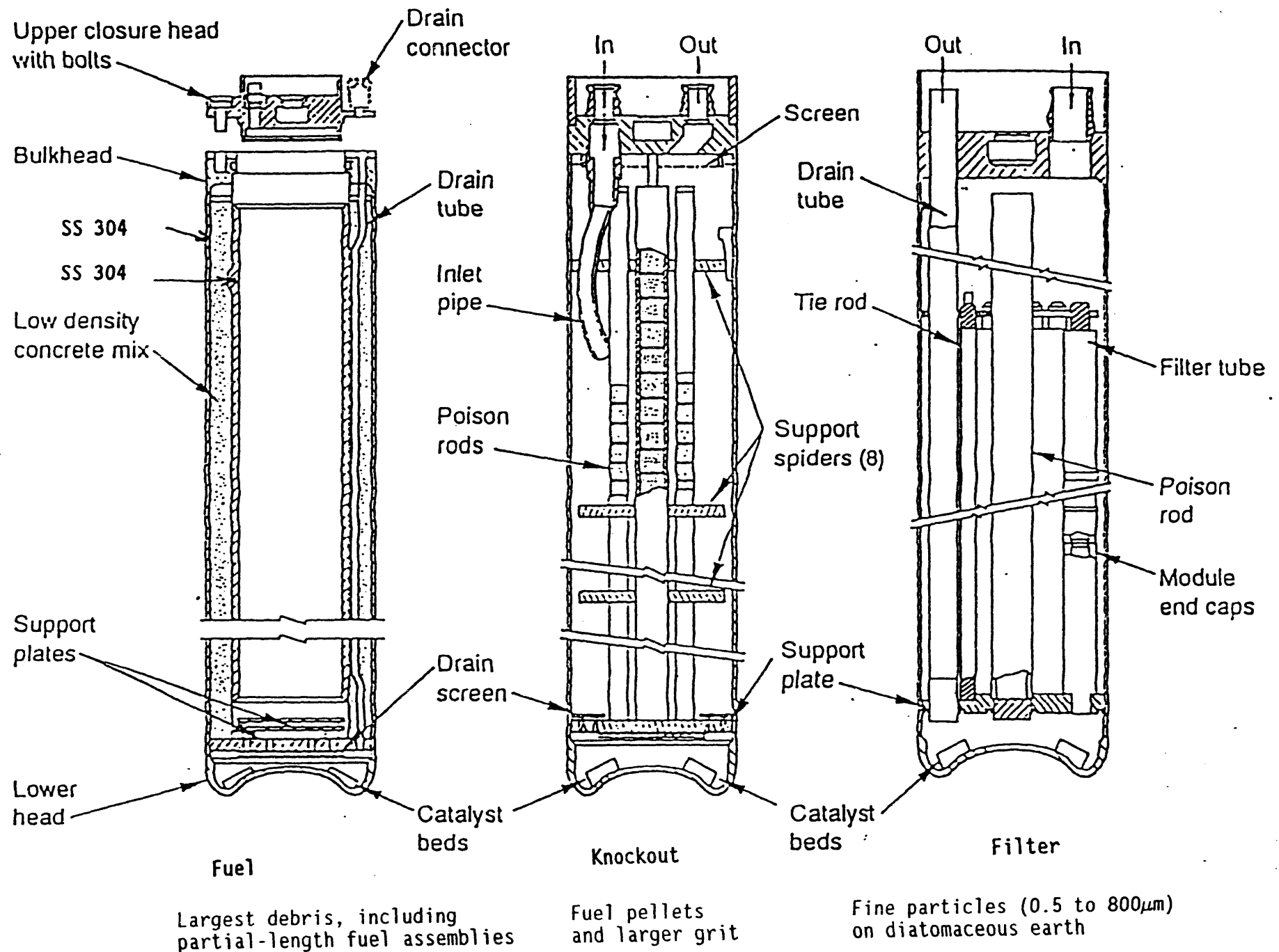
FIGURE 1. Core Debris Canisters
Ref. Schmitt et al. 1993

Fuel

Largest debris, including
partial-length fuel assemblies

Knockout

Fuel pellets
and larger grit

Filter

Fine particles (0.5 to 800μm)
on diatomaceous earth

TABLE 1. Summary of TMI-2 Stainless Steel Canister Environments

	1 TMI-2 Core Waste	2 Canister Loading and Shipping to INEL	3 Storage in TAN Pool	4 Extended Storage
304L SS Fabricated to ASME PVC Sect. VIII; long. & girth welds; no post-weld HT	TMI-2 degraded core in pressure vessel.	Canisters in RPV and in spent fuel pool. Reactor water dosed with H_2O_2. Canisters dewatered; shipped horizontal on rail cars.	Canisters filled with DIW. Make-up from TAN pool to offset evaporation.	Concrete cask, mild steel liner.
	1979	1986	1990	2000
Canister Outside Surface Environments		TMI-2 core water: 4500-4800 ppm B (H_3BO_3); NaOH (pH control) T:20-30°C; 0.5 to 1.9 ppm Cl^-; O_2-saturated.	TAN pool water: T: 20-25°C; 2 ppm Cl^-; O_2-saturated	20°C in water or air. 2 ppm Cl^- in H_2O; O_2-saturated.
Canister Inside Surface Environments		TMI-2 core water; 10^3 R/hr gamma; 0.5 to 1.9 ppm Cl^-; O_2-saturated. Air during shipping; ~13 lb. TMI-2 H_2O left after dewatering.	TAN pool water: T: 20-25°C; Cl^- 2 ppm; O_2-saturated	options for SS canister interiors: a) rinse in DIW; dry 100 hr at 150°C or b) leave filled with water.

DIW: deionized water
HT: heat treatment
RPV: reactor pressure vessel

2.0 THERMODYNAMIC BASIS

When carbon steel is place in water, iron atoms from the metal enter the water by the anodic (electron-donating) reaction:

$$Fe \leftrightarrow Fe^{++} + 2e^- \tag{1}$$

forming a solution of positively charged Fe^{++} ions in the water and giving up two electrons. The electrons enter the metal and need to be removed by a cathodic (electron-accepting) reaction. There are a number of cathodic reactions that can take place at the aqueous solution/metal interface. Two common reactions are: the oxygen reduction reaction

$$O_2 + 2H_2O + 4e^- \leftrightarrow 4(OH)^- \tag{2}$$

and the hydrogen evolution reaction

$$2H^+ + 2e^- \leftrightarrow H_2 \tag{3}$$

Corrosion of iron (or any metal) in contact with an aqueous solution is electrochemical in nature. That is, it is accompanied by release of electrons according to Reaction 1 or a similar reaction, as demonstrated by the fact that the piece of iron acquires an electrochemical potential when immersed in water and that this potential can be readily measured using a voltmeter to determine the voltage between the metal and another reference metal immersed in the same body of water. The presence of the hydrogen evolution reaction is often indicated by bubbles of a gas rising from the corroding metal. The presence of the oxygen reduction reaction may be verified by checking the pH of the water. As may be seen from Reaction 2, the concentration of $(OH)^-$ ions in the water will increase, and the water's pH will increase as the reaction proceeds.

Further, as one would expect of any chemical or electrochemical reaction, Reactions 1 through 3 and other similar corrosion reactions are governed by laws of chemical equilibria, among them the law of mass action. As a result, these reactions may proceed from left to right, or vice versa, by applying an electrical potential to the electrode. Also, as seen from Reactions 1 and 2, since they include H^+ and $(OH)^-$ ions, one can draw plots of electrical potential of a corroding metal against the pH of water on which only certain reactions or reaction products are stable within particular regions of the plot. Such plots are complicated and difficult to calculate for real systems of impure metals corroding in water solutions containing many different ionic species, all of which might take part in reactions similar to those above. However, such plots can be made for the simple system of a single pure metal (such as iron) in contact with the purest electrolyte, water that does not contain any other impurity except dissolved oxygen or hydrogen. Such plots are called potential-pH, or Pourbaix, diagrams. Despite the theoretical nature of such diagrams and the simple metal-pure water systems for which they are plotted, they are of enormous practical importance. For example, most carbon steels are in effect nearly pure iron, containing not more than one weight percent of impurities. Carbon steels, therefore, behave

6

nearly as pure iron, and their behavior under conditions of varying pH and dissolved oxygen content may be predicted, at least qualitatively, from the Pourbaix diagram for iron. This diagram is presented as Figure 2.

Illustrated in Figure 2 are the potential regions for Reaction 1 which are represented by the regions of potential more positive than those shown for lines 23, 13, and 24 (shown by circled numbers). Reactions 2 and 3 can occur only at potentials more negative than those shown for dotted lines b and a, respectively. In other words, iron will only corrode in the region of potentials bounded by lines 23, 13, and 24 on one side and line b if the cathodic reaction is Reaction 3, and by the region bounded by lines 23, 13, and 24, and line a if the cathodic reaction is Reaction 2. Also, between pH's of 9 to 13.5, iron corrodes to form the oxide magnetite, Fe_3O_4 , which generally retards the supply of dissolved oxygen and/or hydrogen ions to the metal surface. The metal then acquires passivity--in principle it is not immune to corrosion but it might acquire immunity because of the formation of a passive film of magnetite on the metal surface. Chloride ions are very small, have high mobility, and because of their negative charge, are attracted toward the positively charged corroding surface (positively charged, because it is shedding positively charged iron ions into the water). These chloride ions locally destroy passive films, even the very tight and dense films that form on stainless steels. The sites of film destruction become potential sites for pit initiation and growth.

In Figure 2, line a, representing the hydrogen evolution reaction, lies above lines 23, 13, and 24 for oxidation of iron. Thermodynamically, this placement dictates that iron is unstable in the presence of water over the entire pH range from -2 to 16, and will corrode with hydrogen evolution. However, though this reaction is thermodynamically possible, the rates of the corrosion reactions are determined by kinetic factors, and often need to be determined empirically.

In summary, thermodynamic considerations indicate that corrosion of the carbon steel liners will proceed under conditions expected to exist during extended interim storage.

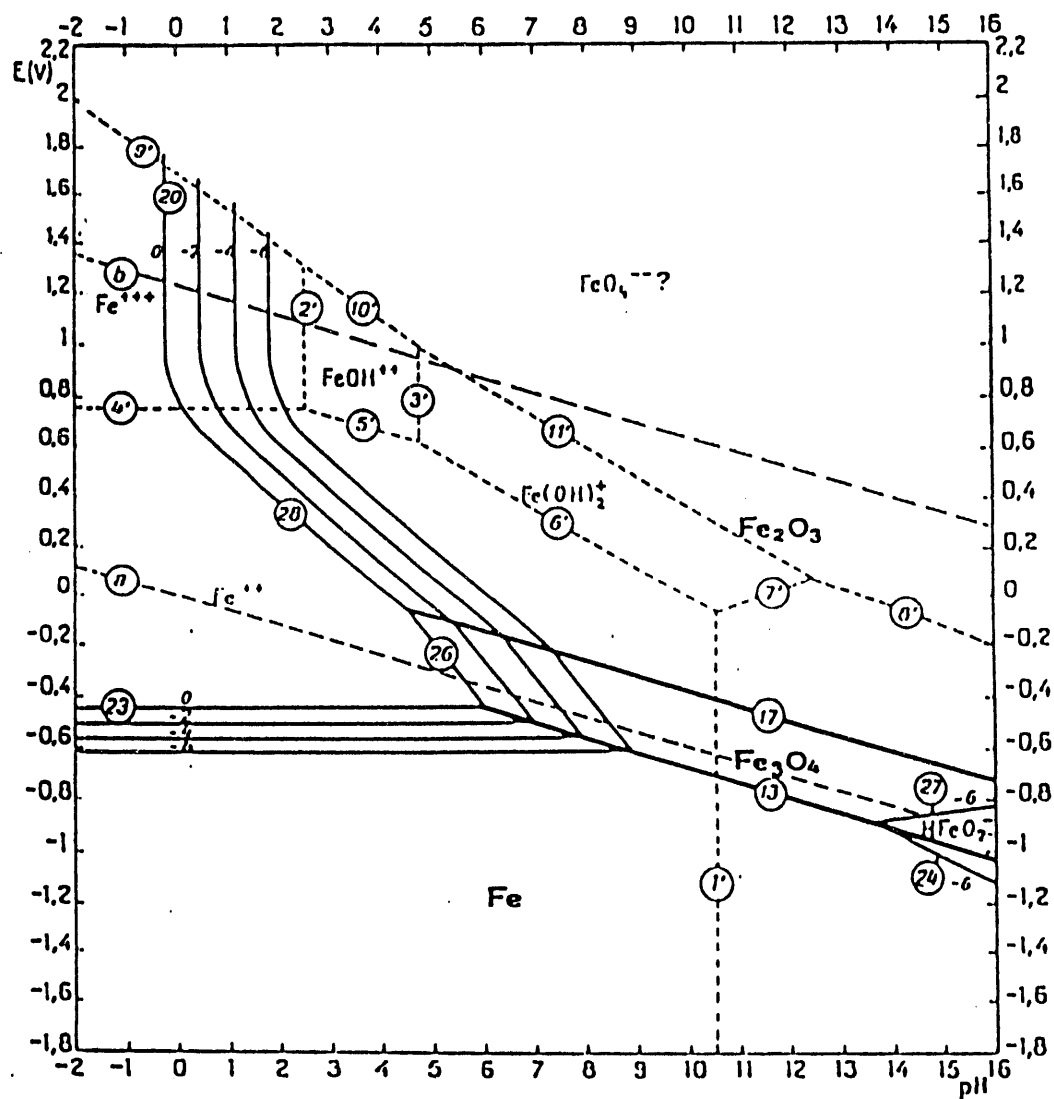FIGURE 2. Potential pH Equilibrium Diagram for the System
Iron Water at 25°C (considering as solid
substances only Fe, Fe_3O_4, and Fe_2O_3).
Ref. Pourbaix, M. 1978. <u>Atlas of
Electrochemical Equilibration in Aqueous
Solutions</u>. McGraw-Hill, pp. 315-318.

3.0 MATERIALS, DESIGNS, AND CONDITIONS

It is essential to this materials evaluation to understand the properties and configurations of the materials that are to be assessed. This section provides a summary of these factors.

3.1 MATERIALS

The canister and storage cask materials are summarized in Table 2. Table 3 provides alloy compositions. The canisters were manufactured according to the 1983 ASME Boiler and Pressure Vessel Code, Section VIII, Division 1. The canisters have longitudinal and girth welds. There was no post-weld heat treatment. On one hand, the absence of the heat treatment will minimize sensitization of the stainless steel, but, on the other hand, the residual stresses of the 304L stainless steel will remain at a high level, assumed to be near the yield strength.

The concrete storage casks include several materials (Table 2), but this analysis will focus on the carbon steel liner.

3.2 DESIGNS

There are three canister designs (Figure 1). Different ranges of debris sizes are stored in the three canisters as indicated in Figure 1. The concrete cask configuration has not been finalized. Currently the concept involves a reinforced concrete cask with a carbon steel liner and carbon steel pipes that would house the stainless steel canisters.

3.3 CONDITIONS

The conditions that the canisters have been exposed to and are expected to be exposed to in the future are summarized in Table 1. Corrosion data applied to estimate durability of the TMI-2 canisters over the time frame 1986 through 2000 (Section 4) were taken from the same sources used for corrosion calculations beyond the year 2000 (Section 5). The results are summarized in the following sections.

9

TABLE 2. Canister and Cask Materials and Dimensions[a]

Component	Material	Dimensions	Fabrication Basis	Remarks
TMI-2 canisters	304L SS	1 ft 2 in. OD 11 ft 8.4 in. height 0.25 in. wall thickness	ASME PVC Section VIII	three canister designs (see Figure 1)
concrete casks	reinforced concrete	8 ft 9 in. OD 15 ft 5.5 in. height		exterior sealant on concrete; Al alloy plate on cask lid; carbon steel shield plug
	carbon steel cask liner, alloy ASTM A516 Gr60	wall thickness: 3 in. floor thickness: 0.75 in.		
	carbon steel pipes; alloy ASTM A53 GrB	16 schedule 40 pipes 16 in. OD 15.1 in. ID 12 ft 10.5 in. height		

(a) Schmitt et al. 1993

TABLE 3. Composition of Carbon Steel Cask Liner and Stainless Steel Canister Materials[a]

Steel Alloys	C	P	S	Mn	Si	Other
ASTM A36 (UNS K02600)	.26 max	.04 max	.05 max			.20 Cu (when Copper Steel is specified)
ASTM A516 gr. 60 (UNS K02100)	.21 max	.035 max	.04 max	.55 - .98	.13 - .45	
ASTM A53 gr. B (UNS K03005)	.30 max	.05 max	.06 max	1.20 max		

Stainless Steel Alloys	C	Cb/Nb	Co	Cr	Cu	Mn	Mo	N	Ni	P	S	Si	Ta	Ti	V
ASME SA 240 - 304L (UNS S30403)	.03 max			18.00 - 20.00		2.00 max			8.00 - 12.00	.045 max	.030 max	1.00 max			
308L (Coated Electrode for Stainless Steel)	0.019 - 0.032	0.01	0.03 - 0.13	19.81 - 20.31	0.03 - 0.16	1.56 - 2.1	0.02 - 0.30	0.035	9.82 - 10.3	0.016 - 0.02	0.004 - 0.01	0.34 - 0.51	0.01	0.001 - 0.02	0.064 - 0.116

(a) Schmitt et al. 1993

11

4.0 ESTIMATED TMI-2 CANISTER DURABILITY: 1986 - 2000

This section addresses durability estimates for the TMI-2 canisters during loading and wet storage at TMI, shipping, and wet storage at INEL for the period 1986 to 2000 (see Table 1).

The corrosion assessments for the 1986 - 2000 time frame included consideration of both uniform and localized mechanisms. The exposure conditions for the type 304L canisters at TMI-2 and at INEL are summarized in Table 1, involving temperatures near 20-30°C, Cl⁻ ~2 ppm, and O_2-saturated water. Because the conditions in the time frame 1986 to 2000 are similar to conditions specified for the aqueous case beyond 2000, the same corrosion data were used. The data and rationales appear on data sheets for matrices A and D that are shown in Table 4 for the evaluation of corosion beyond the year 2000.

From the Matrix D data sheet, the general corrosion rate for 304L SS in water is 0.012 mils/y, applied over 14 y. Other corrosion phenomena in water are indicated to be nil in the same time frame, based on data in Section 5, Matrix A data sheet. The durability results in water are summarized below:

general corrosion	0.17 mils
stress corrosion cracking	nil
pitting corrosion	nil
galvanic corrosion	nil
crevice corrosion	nil

A metallographic study of stainless steel components exposed in spent fuel pools for periods up to 15 y (Kustas et al. 1981) offers confirmatory evidence for the results summarized above. Subject to uncertainties in interpreting metallographic sections on high-integrity materials, the sections suggest that significant localized corrosion was absent, except for occasional mild intergranular corrosion near welds on 304 SS, where sensitization can occur.

Another study (Bruemmer and Johnson 1983) offers a basis to judge effects of welding on sensitization of the 304L canisters. In the study, type 304L SS was subjected to a 625°C/24 hr heat treatment; three type 304 SS materials were subjected to the same thermal conditions (Bruemmer and Johnson 1983). Degrees of sensitization for the four materials were compared using electrochemical potentiokinetic reactivation (EPR) measurements. The EPR values varied from 1.4 Coulombs per square centimeter (C/cm²) for 304L material to 35.2 C/cm² for the most sensitized 304 material. For unsensitized material the EPR values would be 0.0 to 0.5 C/cm². The thermal treatment used in the study is more severe than is likely to occur in welding. The study was conducted in oxygen-saturated water with 15 ppm Cl⁻ at 32°C. Absence of cracking on "sensitized" type 304L specimens in the study strongly suggests that weld sensitization will not promote SCC of the 304L canisters. The

influence of stress in the study also mitigates prospects that SCC will occur. Residual stresses in the unannealed canisters are assumed to be near yield stresses, in lieu of specific evidence. In the referenced test series, no cracking occurred if the stress level was below 180% of the yield stress. The combination of low levels of weld-induced sensitization and stress levels below the expected threshold for SCC suggests that SCC of the type 304L TMI-2 canisters will be nil.

5.0 ESTIMATED TMI-2 CANISTER AND LINER DEGRADATION BEYOND 2000

Results of corrosion assessments for extended interim storage of the TMI-2 canisters and related behavior of the steel cask liners are summarized in Table 4. The matrix addresses 304L SS and 1020 CS in three environments and includes consideration of general and localized corrosion, resulting in twelve data fields, A through L. Table 4 is followed by summaries that include conditions and rationale for corrosion assessments in each data field (Matrices). The term pinhole penetration is defined as a small hole that penetrates completely through the canister wall or the carbon steel liner. The pinhole can occur by several corrosion mechanisms, including pitting, stress corrosion cracking, or crevice corrosion.

The requested assessment included definition of the time to 50% loss of strength. This was interpreted to be represented by 50% wall loss by uniform corrosion (50% loss in Table 4). The wall thinning is assumed to occur from the outer canister surfaces. The _fuel_ canisters have double containment (Figure 1). The canisters will either be dried and filled with air or will remain filled with water as they are placed in extended interim storage.

TABLE 4. Summary of Corrosion Estimates[a] Beyond 2000 AD

Materials	Environment		
	H$_2$O 20°C	Air + 10% RH	Air + 40% RH
304 SS canisters (pinholes)	**Matrix A** penetration by pitting: nil scc: nil crevice corrosion: nil galvanic corrosion: nil	**Matrix B** penetration by pitting: nil scc: nil crevice corrosion: nil galvanic corrosion: nil	**Matrix C** penetration by pitting: nil scc: nil crevice corrosion: nil galvanic corrosion: nil
304 SS canisters (50% wall thickness loss)	**Matrix D** wall thinning: 4600 y	**Matrix E** wall thinning: 11,500 y	**Matrix F** wall thinning: 11,500 y

carbon steel cask liners (pinholes)	**Matrix G**
	
	penetration by
	pitting: 50 y - 50 mils
	          through-wall 750 y
	scc: nil
	crevice corrosion: ~50 mils
	galvanic corrosion: nil
		Matrix H
		
		penetration by
		pitting: 50 y - 5 mils
		        through-wall: 7500 y
		scc: nil
		crevice corrosion:>7500 y
		galvanic corrosion: nil
			Matrix I
			
			penetration by
			pitting: 50 y - 10 mils
			          through-wall: 3800 y
			scc: nil
			crevice corrosion: >3800 y
			galvanic corrosion: nil

carbon steel cask liners (50% wall thickness loss)	**Matrix J**
	
	wall
	thinning: 50 y - 50 mils
	          50% loss - 375 y
		Matrix K
		
		wall
		thinning: 50 y - 5 mils
		          50% loss - 3800 y
			Matrix L
			
			wall
			thinning: 50 y - 10 mils
			          50% loss - 1900 y

15

(a)   See following data sheets for data sources, corrosion rates and calculations, and rationales. The data sheets are coded to the matrix fields in Table 4.

<u>Matrix A</u>

1. Scope: Type 304L stainless steel, pinhole penetration

2. Component: Core debris canister

3. Conditions: Water at 20°C, gamma flux 1000 R/h, 2 ppm Cl⁻, O_2-saturated

4. Data Source(s):

    A.1 Szklarska-Smialowska, Z. <u>Pitting Corrosion of Metals</u>. NACE, Katy, Texas, p. 243 & 245. 1986.

    A.2 Bruemmer, S. M., and A. B. Johnson, Jr. "Effect of Chloride, Thiosulfate, and Fluoride Additions on the IG SCC Resistance of Type 304 Stainless Steel in Low Temperature Water." <u>Proceedings of the International Symposium on Environmental Degradation of Materials in Nuclear Power System--Water Reactors</u>. Published by National Association of Corrosion Engineers. American Nuclear Society, Myrtle Beach, South Carolina, pp. 571-580. 1983.

    A.3 Metals Handbook, Ninth Edition, p. 977, 1987.

5. Corrosion Rate: 0 mil/y

6. Corrosion Calculation: (219 mil)[a] ÷ (0 mil/y) = infinite time to failure

7. Rationale: <u>Pitting</u>: On the basis of a critical evaluation of available literature, it is strongly believed that pitting of Type 304L stainless steel will not occur under the specified conditions. A brief summary of the literature review that led to the above conclusion follows.

    The most negative potential for nucleation of pits[b], E_{np}, on austenitic stainless steels measured in chloride bearing waters at room temperature is +0.135 V SCE. Assuming the corrosion potential, Ecorr, to be no more positive than -0.35 V SCE in aerated chloride solutions of neutral pH (pH=6 to 9), the potential will have to be raised by 0.135-(-0.350) = 0.485 V for pitting to occur. Usually pitting is initiated when points on a stainless steel surface become enriched in chloride ions (Cl⁻), and the chromium-rich oxide film on the surface is locally destroyed. Conditions that favor pit initiation are high temperatures, high chloride concentration, low pH values, the presence of deposits or debris on the metal surface, oxygen impoverishment, and stagnant conditions (A.1). In the case of the TMI-2 canisters, the neutral pH of

---

(a) The general wall thickness is 250 mil; the bottom head thickness is 219 mil, representing the thinnest wall section.

(b) See Section 2: THERMODYNAMIC BASIS, for a discussion of corrosion terms and basics.

water, the very low halide concentrations (2 ppm Cl⁻), and the presence of oxygen in water (saturated with air, hence containing about 8 ppm dissolved oxygen) are all factors that do not favor pit initiation and growth. Factors that would encourage pitting are the stagnant water and gamma radiation. Gamma radiation of the anticipated magnitude (1000 R/h) is expected to make Ecorr more positive by not more than 0.1 V, since literature data (A.1) indicate that a radiation level of 10^6 R/h leads to a potential change of +150-200 mV in low chloride (7 ppm Cl) water. The anticipated increase in Ecorr will raise it to a level which will still be far below E_{np}. On the other hand, the rise of Ecorr is due to generation of oxidizing species in the solution. Since initiation and propagation of pits is due to oxygen depletion at pitting sites, the presence of radiation will tend to counteract oxygen depletion. Finally, no documented instances of pitting of 18Cr-Ni stainless steels have been discovered for aqueous solutions at chloride contents of below 100 ppm.

Stress Corrosion Cracking: Types 304 and 304L SS were subject to sensitizing heat treatments and then were tested at constant axial load in aerated DIW with ranges of Cl⁻, F⁻, and $S_2O_3^=$. No cracking was observed, even for moderately sensitized specimens in water with 15 ppm Cl⁻ if the applied stress was less than 180% of yield (A.2).

Crevice Corrosion: The crevice factor for carbon steel at 50°C in Tuff groundwater was ~1 (A.3). The crevice factor for stainless steel is not expected to be substantially different.

Galvanic: Galvanic couple effects are not expected to be of concern for 304L stainless steel; the material is noble to carbon steel and would not be expected to preferentially corrode.

<u>Matrix B</u>

1. Scope: Type 304L stainless steel, pinhole penetration

2. Component: Core debris canister

3. Conditions: 20°C, air at + 10% RH, gamma flux 1000 R/h

4. Data Source(s):

   B.1 Dean, S. W., and T. S. Lee, eds. <u>Degradation of Metals in the Atmosphere</u>. ASTM STP 965, 1987 (Pitting Data).

   B.2 Baboian, R., et al., eds. <u>Galvanic and Pitting Corrosion</u>. ASTM STP 576, 1976 (Galvanic Data).

   B.3 LaQue, F. L., and H. R. Copson. <u>Corrosion Resistance of Metals and Alloys</u>. 2nd ed. Reinhold Publishing Corp. 1963.

   B.4 Fontana, M. G., and N. D. Greene. <u>Corrosion Engineering</u>. 2nd ed. McGraw-Hill Book Co., 1978 (Crevice Data).

   B.5 <u>Behavior of Stressed and Unstressed 304L Specimens in Tuff Repository Environmental Conditions</u>. UCRL-91804, Lawrence Livermore National Laboratory Report, November 1984 (SCC Data).

5. Corrosion Rate: 0 mil/y

6. Corrosion Calculation: Time to through-wall penetration for nominal wall thickness, bottom head = 219 mils

   (219 mils) ÷ (0 mil/y) = infinite time to failure

7. Rationale: <u>Pitting</u> - See Matrix A rationale for discussion of pitting on 304L stainless steel. Long-term (26-y) atmospheric studies conducted on type 304L in a marine environment 250 meters from the ocean at Kure Beach test sites in North Carolina yielded corrosion rates of <0.4 mpy. Pitting and crevice corrosion are localized forms of corrosion that are accelerated by the presence of halides such as Cl^- in the environment, and the levels of Cl^- are high in an atmospheric marine environment. Atmospheric marine environments present a more aggressive environment for the material than the canister environment, due to variable humidity conditions, variable temperature conditions, and variable amounts of atmospheric pollutants. The corrosion rate for the 304L in the aggressive environment remained low over a long period of study, so it is reasonable to assume that the material would exhibit even lower rates of corrosion in long term usage in a more benign TMI-2 canister environment. This approach using atmospheric corrosion data has been supported by reports such as UCRL-53449 "Containment Barrier Metals for High-Level Waste Packages in a Tuff Repository" by Russell et. al. dated October 12, 1983. It is noted by LaQue and Copson (B.3) that if the relative humidity remains below 30% for the environment in question, the

corrosion of most metals is negligible. They also mention that the surface should be kept reasonably clean of hygroscopic "dirt" which can cause corrosion even at 20% relative humidities.

Crevice - Crevice corrosion can arise from a difference in oxygen concentration leading to a differential oxygen cell effect. This effect is more pronounced for areas under water droplets or dirt, so at the low relative humidity conditions this type of corrosion is not expected to contribute substantially to the corrosion rates.

Stress Corrosion Cracking - Stress corrosion cracking requires three crucial conditions to be satisfied in order for the material to crack in the environment in question. These three conditions are a susceptible microstructure, an applied or residual stress, and corrosive environment. There is evidence that the microstructure has not been sensitized to the point of making the material susceptible to SCC (Bruemmer and Johnson 1983), and the environment at 20°C is benign regarding initiation of SCC (see Matrix A rationale and Section 4.0).

Galvanic - Galvanic couple effects are not expected to be of concern for 304L stainless steel; the material is noble to carbon steel and would not be expected to preferentially corrode.

Matrix C

1. Scope: Type 304L stainless steel, pinhole penetration

2. Component: Core debris canister

3. Conditions: 20°C, air at 40% RH, gamma flux 1000 R/h

4. Data Source(s):

   • See references for Matrix A

   C.1 Dean, S. W., and T. S. Lee, eds. Degradation of Metals in the Atmosphere. ASTM STP 965, 1987 (Pitting Data).

   C.2 Baboian, R., et al., eds. Galvanic and Pitting Corrosion. ASTM STP 576, 1976 (Galvanic Data).

   C.3 LaQue, F. L., and H. R. Copson. Corrosion Resistance of Metals and Alloys. 2nd ed. Reinhold Publishing Corp. 1963.

   C.4 Fontana, M. G., and N. D. Greene. Corrosion Engineering. 2nd ed. McGraw-Hill Book Co., 1978 (Crevice Data).

   C.5 Behavior of Stressed and Unstressed 304L Specimens in Tuff Repository Environmental Conditions. UCRL-91804, Lawrence Livermore National Laboratory Report, November 1984 (SCC Data).

5. Corrosion Rate: 0 mil/y

6. Corrosion Calculations: Time to through-wall penetration nominal wall thickness bottom head = 219 mils

   (219 mils) ÷ (0 mil/y) = infinite time to failure

7. Rationale: Pitting - See Matrix B rationale.

   Crevice - See Matrix B rationale.

   Stress Corrosion Cracking - See Matrix B rationale.

   Galvanic - See Matrix B rationale.

Matrix D

1. Scope: Type 304L stainless steel, 50% wall thickness loss

2. Component: Core debris canister

3. Conditions: 20°C, Air-Saturated Water (dissolved oxygen ~8 ppm), gamma flux 1000 R/h, 2 ppm Cl⁻

4. Data Source(s):

    D.1 McCright, R. D., et al. "Selection of Candidate Canister Materials for High Level Nuclear Waste Containment in a Tuff Repository." Corrosion '84, Paper 198, April 2-6, 1984, New Orleans, Louisiana.

    D.2 Weiss, H., et al. Metallurgical Analysis of a 304L Stainless Steel Canister from the Spent Fuel Test --- Climax. UCID-20436, Lawrence Livermore National Laboratory Report, April 1985.

5. Corrosion Rate: unirradiated - 0.01 mil/y (1 out of 3 coupons) <0.005 mil/y (2 out of 3 coupons), weight loss detection limit (D.1)

    irradiated (3 x 10⁵ rad/hr) - 0.012 mil/y (D.1)

6. Corrosion Calculations: Time to 50% wall thickness loss

    (219/2 mil) ÷ (2 x 0.012 mil/y) = 4600 y (rounded) (corrosion from ID and OD surfaces)

7. Rationale: The unirradiated specimen corrosion rates represent measured uniform corrosion rates in tuff groundwater at 100°C for 1000-hour test exposures. The irradiated specimen corrosion rates represent measured rates in tuff groundwater at 105°C for 2-month test exposures. The tuff groundwater composition is a relatively benign environment with a Cl⁻ concentration of 7.5 ppm (as compared to the 2.0-2.5 ppm level in the TAN water). A complete breakdown of the water composition is given in data source D.1. The test environments are aggressive when compared to the reference environment for this study, due to the increased corrosion rate that can be expected from the increase in temperature. This is also the case for the higher radiation levels used in the test cited above when compared to the radiation levels at the surface of the fuel debris canisters. The corrosion rates will be very conservative due to the discrepancy between test conditions cited in the above reference and expected conditions for the TMI-2 fuel canisters with respect to temperature and radiation levels.

    Described in data source D.2, the metallurgical analysis of a 304L canister after it was used to store spent fuel from Turkey Point Unit #3 reactor in a high level nuclear waste repository demonstration in climax granite. The storage configuration was essentially the same as the proposed configuration for the TMI-2 waste canisters: a 304L canister

used to contain the waste, surrounded by a carbon steel liner. Water entered the waste package between the carbon steel liner and the 304L canister because of a crack in the carbon steel liner. From temperature measurements by thermocouples on the liner and the canister, the water was estimated to be present for approximately 3 years and the water contained from 6.9 to 160 mg/L Cl^-. The report stated that the canister material suffered no observable corrosion or cracking for the 3-year period. This environment is also more aggressive due to higher radiation levels of the Turkey Point spent fuel assemblies, the associated higher temperatures, and higher Cl^- concentrations.

Matrix E

1. Scope: Type 304L stainless steel, 50% wall thickness loss

2. Component: Core debris canister

3. Conditions: 20°C, Air + 10% RH, gamma flux 1000 R/h

4. Data Source(s):

    E.1 Russell, et al. Containment Barrier Metals for High-Level Waste Packages in a Tuff Repository. UCRL-53449, Lawrence Livermore National Laboratory Report, October 1983.

    E.2 LaQue, F. L., and H. R. Copson. Corrosion Resistance of Metals and Alloys. 2nd ed. Reinhold Publishing Corp., 1963.

    E.3 Effect of Ionizing Radiation On Moist Air Systems. UCRL-97936, Lawrence Livermore National Laboratory Report, December 1987.

5. Corrosion Rate: 0.005 mil/y (E.1)

6. Corrosion Calculation: Time to 50% wall thickness loss

    $(219/2 \text{ mil}) \div (2 \times 0.005 \text{ mil/y}) = 11,500 \text{ y}$ (corrosion from ID and OD surfaces)

7. Rationale: The above corrosion rates are based on 304 SS atmospheric corrosion rates during a 5-year exposure at an industrial site in the United Kingdom with air pollution controls and a mean temperature of 15°C. The uncertainty associated with basing the corrosion rates on these data stem from the temperature fluctuations, humidity fluctuations, and a low but variable amount of atmospheric pollutants. The specimens were not subject to a radiation field, but the radiation flux in moist air is expected to result in nitric acid formation. Stainless steel is known to passivate in the presence of nitric acid, so the corrosion rate is not expected to increase. It is noted by LaQue and Copson (E.2) that if the relative humidity remains below 30%, general corrosion of most metals is negligible.

Matrix F

1. Scope: Type 304L stainless steel, 50% wall thickness loss

2. Component: Core debris canister

3. Conditions: 20°C, Air at 40% RH, gamma flux 1000 R/h

4. Data Source(s):

    F.1   Russell, et al. Containment Barrier Metals for High-Level Waste
           Packages in a Tuff Repository. UCRL-53449, Lawrence Livermore
           National Laboratory Report, October 1983.

    F.2   LaQue, F. L., and H. R. Copson. Corrosion Resistance of Metals
           and Alloys. 2nd ed. Reinhold Publishing Corp., 1963.

    F.3   Effect of Ionizing Radiation On Moist Air Systems. CRL-97936,
           Lawrence Livermore National Laboratory Report, December 1987.

5. Corrosion Rate: 0.005 mil/y (F.1)

6. Corrosion Calculations: Time to 50% wall thickness loss

    (219/2 mil) ÷ (2 x 0.005 mil/y) = 11,500 y (corrosion from ID and
    OD surfaces

7. Rationale: The above corrosion rates are based on 304 SS atmospheric
    corrosion rates during a 5-year exposure at an industrial site in the
    United Kingdom with air pollution controls, with a prevailing
    temperature of 15°C. The uncertainty associated with basing the
    corrosion rates on these data stem from the temperature fluctuations,
    humidity fluctuations, and a low but variable amount of atmospheric
    pollutants. The specimens were not subject to a radiation field, but
    the radiation flux in moist air is expected to result in nitric acid
    formation. Stainless steel is known to passivate in the presence of
    nitric acid, so the corrosion rate is not expected to increase.

1. Scope: Type 1020 carbon steel, pinhole penetration

2. Component: Cask liner

3. Conditions: 20°C, air-saturated water (dissolved oxygen ~8 ppm), gamma flux 1000 R/h, 2 ppm Cl⁻.

4. Data Source(s):

    G.1   Pourbaix, M.   Atlas of Electrochemical Equilibria in Aqueous Solutions. NACE, Houston, Texas, p. 313. 1974.

    G.2   Fontana, M. G., and N. D. Greene. Corrosion Engineering. McGraw-Hill, p. 161. 1978.

    G.3   Szklarska-Smialowska, Z. Pitting Corrosion of Metals. Houston, Texas, p. 203. 1986.

    G.4   Parkins, R. N. "Stress Corrosion Cracking of Low Carbon Steels." In Fundamental Aspects of Stress Corrosion Cracking. Eds. R. W. Staehle, A. J. Forty, and D. Van Rooyen, pp. 361-373. 1969.

    G.5   Galvanic Metals Handbook, p. 977.

    G.6   Fontana and Greene, ibid, p. 35.

5. Corrosion Rate: 1 mil/y

6. Corrosion Calculations:

    a) penetration at 50 y: (1 mil/y) x (50 y) = 50 mils

    b) time to complete penetration: (750 mil) ÷ (1 mil/y) = 750 y

7. Rationale: ASTM A516 gr 60 steel (C 0.21% max, Mn 0.55-0.98%, Si 0.13-0.45%), the cask liner material is similar in composition to SAE 1020 steel (C 0.18-0.23%, Mn 0.30-0.60%). It will have corrosion properties similar to other low-carbon (<0.3% C) steels. Carbon steels in general will pit in waters containing halides (fluoride, chloride, bromide, and iodide) and under conditions where differential aeration cells (different concentrations of dissolved oxygen, as in the case of the outside and inside of a crevice or a gasket). However, a minimum concentration of a halide ion is necessary for these ions to undermine the protective oxide film that generally forms on steels in aqueous solutions at pH values between 6 and 13. This film may be only a few atoms thick and not always visible. The halide ions, if in sufficient concentration, destroy the passive film locally, initiating a pit at the site. If the concentration is below the minimum, pitting does not occur, but the general corrosion rate might increase (G.3). The minimum chloride concentration for room-temperature aqueous solutions for

pitting of iron is reported to be 11 ppm at pH 0 (acid solutions), 18 ppm at pH 5 (near-neutral acid solutions), and 106 ppm at pH 8.4 (basic solutions). The pH of the storage water is expected to be near neutral, differential concentration cells are expected to be minimal due to the oxidizing effect of extant radiation of 1000 R/h, also the chloride content (2 ppm) is well below that at which pitting will occur, even in acid solutions; therefore, pitting of carbon steel is expected to be minimal during storage. The expected pitting rate is estimated to be equal to the general corrosion rate, estimated to be no more than 1 mil/y (see Matrix J).

Stress Corrosion Cracking: Carbon steel is expected to be resistant to stress corrosion cracking under the relatively benign conditions expected for the cask liners (G.4).

Other concerns regarding pinhole penetration are 1) crevices under the dished end of canisters, and 2) galvanic effects at points of contact with the stainless steel canister. Crevice corrosion occurs from the cumulative effect of several phenomena occurring in crevices, including oxygen depletion because corrosion reactions within the crevice deplete oxygen, while the exterior supply is limited due to lack of circulation of the solution; a second phenomenon is acidification of the crevice solution because of hydrolysis of metal ions going into solution (e.g., $Fe^{++} + 2H_2O \rightleftharpoons Fe(OH)_2 + 2H^+$); a third phenomenon is migration of negatively charged Cl^- ions into the crevice containing an excess of positively charged H^+ ions. Crevice corrosion is not expected to occur in the present case due to the small chloride concentrations of the cask environment and the presence of radiation at 1000 R/h, causing radiolysis, which is expected to counteract effects of oxygen depletion. Galvanic effects (G.5) lead to corrosion when a corrosion resistant material is in electrical contact with a corrosion prone material. The usual result of galvanic corrosion is that the corrosion resistant material corrodes at an even lower rate than it would have when isolated, and the corrosion-prone material corrodes at a higher rate. The effect on rates is larger, the larger the area of the more noble metal. In the present case, galvanic effects are expected to be minimal because of the noncorrosive nature of the water, nearly equal areas of contact between relatively noble Type 304L stainless steel canister and relatively more corrosion prone carbon steel, and the oxidizing effect of radiation. The radiation is expected to decrease the galvanic effect by raising the corrosion potential of both metals. Because stainless steel is easily polarized, galvanic effects on other metals often tend to be minimized.

Matrix H

1. Scope: Type 1020 carbon steel, pinhole penetration

2. Component: Cask liner

3. Conditions: 20°C, Air at 10% RH

4. Data Source(s):

   H.1   Abbott, W. H. Unpublished Results. Private Communication, March 16, 1994, Battelle Columbus Laboratories.

5. Corrosion Rate: 0.1 mil/y (H.1)

6. Corrosion Calculations:

   a) Penetration in 50 y: (0.1 mil/y) x (50 y) = 5 mils

   b) Time to through-wall penetration: (750 mil) ÷ (0.1 mil/y) = 7500 y

6. Rationale: As described in Matrix K, the corrosion of carbon steel under the above conditions will be immeasurably small for exposures of a few years. Further, the corrosion will be of the uniform type and not of the pinhole type. This is so because, in view of available literature data, there is a minimum relative humidity below which corrosion of metals will not occur. The minimum RH is a function of temperature and contaminants in the air (minimum 50% RH at 10 ppb Cl_2 in air at room temperature). The reported rate from the data source for 1010 carbon steel (0.1% C) is 0.2 mil/y in air of 70% RH and containing 10 ppb Cl_2. We, therefore, assume a conservative rate of half of this rate, 0.1 mil/y, for 10% RH air at 20°C that does not contain chlorine or other contaminants. It is likely that the actual rate will be a fraction of this rate.

Matrix I

1. Scope: Type 1020 carbon steel, pinhole penetration

2. Component: Cask liner

3. Conditions: 20°C, Air at 40% RH

4. Data Source(s):

   I.1 Abbott, W. H. Unpublished Results. Private Communication, March
   16, 1994, Battelle Columbus Laboratories.

5. Corrosion Rate: 0.2 mil/y (I.1)

6. Corrosion Calculations:

   a) Penetration at 50 y: (0.2 mil/y) x (50 y) = 10 mils

   b) Time to through-wall penetration: (750 mil) ÷ (0.2 mil/y) = 3800 y

6. Rationale: See rationale for Matrix H. Air with 40% RH is expected to
be slightly more aggressive than air with 10% RH; therefore, the
corrosion rate was estimated to be 0.2 mil/y.

Matrix J

1. **Scope:** Type 1020 carbon steel, 50% wall thickness loss

2. **Component:** Cask liner

3. **Conditions:** 20°C, Air-Saturated Water, gamma flux 1000 R/h, 2 ppm Cl⁻

4. **Data Source(s):**

   J.1 Pourbaix, M. <u>Atlas of Electrochemical Equilibration in Aqueous Solutions</u>. McGraw-Hill, pp. 315-318. 1978.

   J.2 Glass, R. S., R. A. Van Konynenburg, and G. E. Overturf. <u>Corrosion Processes of Austenitic Stainless Steels and Copper-Base Materials in Gamma Irradiated Aqueous Solutions</u>. UCRL-92941, pp. 1-15, September 1985.

5. **Corrosion Rate:** 1 mil/y

6. **Corrosion Calculation:**

   a) penetration at 50 y: (1 mil/y) x (50 y) = 50 mils

   b) time to 50% wall loss: (750/2 mil) ÷ (1 mil/y) = 375 y

7. **Rationale:** Corrosion rates for carbon steel in aqueous solutions are a function of pH and dissolved oxygen content (J.1). The corrosion rates are small (<0.3 mil/y) for pHs between 9.5 and 12.5, but progressively increase as the pH decreases below 9.5 or increases above 12.5. At pHs above 8.0, the amount of oxygen in oxygen-saturated water (8 ppm at 25°C) is sufficient to form a film of magnetite, Fe_3O_4, on the surface, and the corrosion rate is expected to be close to 0.1 mil/y. At pH values up to pH 8, the presence of oxygen will not bring about the passivation of the surface but instead give a higher corrosion rate, about 1 mil/y. With radiation of 1000 R/h, the potential will rise higher (J.2), probably by about 0.1 V. At pH values above 8, radiation will be beneficial in that it will improve the formation of a passive film, promoting low corrosion rates. The corrosion rates given above are based on data for distilled and potable waters with or without oxygen (J.1).

   Crevice and galvanic effects are considered minimal for reasons presented in Matrix G.

Matrix K

1. Scope: Type 1020 carbon steel, 50% wall thickness loss

2. Component: Cask liner

3. Conditions: 20°C, air at 10% RH

4. Data Source(s):

   K.1 Abbott, W. H. Unpublished Results, <u>Private Communication</u>, March 16, 1994, Battelle Columbus.

5. Corrosion Rate: 0.1 mil/y (K.1)

6. Corrosion Calculations:

   a) penetration at 50 y: (0.2 mil/y) x (50 y) = 5 mils

   b) time to 50% wall thickness loss: (750/2 mil) ÷ (0.1 mil/y) = 3800 y

7. Rationale: The corrosion of metals in air is a function of relative humidity and the kind and amount of impurities present. The most corrosive impurities are nitrogen dioxide (NO_2), sulfur dioxide (SO_2), and chlorine (Cl_2). In the case of SAE 1020 (0.2 percent carbon), at 100 ppb chlorine in air, corrosion rates were 2 mil/y at 80% RH, 0.2 mil/y at 70% RH, and immeasurably small at humidities of 50% RH and lower over an exposure of two years. The corrosion rate of ASTM A515 gr. 60 carbon steel for the above conditions is conservatively estimated to be 0.1 mil/y.

Matrix L

1. **Scope:** Type 1020 carbon steel, 50% wall thickness loss

2. **Component:** Cask liner

3. **Conditions:** 20°C, air at 40% RH

4. **Data Source:** See Matrix H and Rationale below.

5. **Corrosion Rate:** 0.2 mil/y maximum

6. **Corrosion Calculation:**

   a) penetration at 50 y: (0.2 mil/y) x (50 y) = 10 mils

   b) time to 50% wall thickness loss: (750/2 mil) ÷ (0.2 mil/y) = 1900 y

7. **Rationale:** As explained in Matrix H, corrosion rates for carbon steel at 20°C and in air of 40% RH will be negligibly small. They will, however, be larger than at 10% RH. As we conservatively estimated a rate of 0.1 mil/y for Matrix H, a proportional estimate for the rate at 40% RH is double the rate at 10% RH, or 0.2 mil/y.

6.0 DISCUSSION

The projection of materials behavior over centuries and millennia remains a challenging exercise. However, the demonstrated durability of numerous metals and alloys over long time periods (Johnson & Francis 1980) lends some credibility to the assessment, particularly for a material with recognized corrosion resistance (Type 304L SS) exposed to relatively benign conditions. Estimated corrosion penetrations for carbon steel liners seem qualitatively consistent with the described condition of iron artifacts exposed in air for more than three millennia.

A major challenge in this assessment was to identify corrosion data that are fully relevant to the specified environmental regimes. For stainless steels at 20°C in relatively pure waters, corrosion rates are too low to be of practical concern for most applications and, therefore, have not been the subject of substantial study. Consequently, data from more aggressive regimes had to be adapted. The basis for the carbon steel corrosion assessment was approached similarly. Therefore, the projected degradation rates are likely to be conservative. Extrapolations, e.g., from higher to lower temperatures, could possibly have increased the relevancy, but some data (Robertson 1991) suggest that temperature effects for stainless steel corrosion become nil at lower temperatures, if the materials is passive.

Again, there is little incentive to measure carbon steel or stainless steel corrosion rates in pure air at 20°C. Therefore, the principal long-term data sources are from atmospheric corrosion studies in air with some pollutants, with a range of temperatures, and humidity levels that at times may exceed the 10-40% RH range. These assessments also are expected to provide conservative results.

There are several uncertainties, e.g., regarding the debris configurations inside the canisters that could promote occluded cell attack. Also, the scope of the effort did not permit in-depth consideration of effects of the radiation field on corrosion. However, some insights to radiation effects are available in the literature and do not portend large accelerations.

The higher corrosion rates for carbon steel will result in an inventory of iron oxides that will have substantial mobility, at least while oxygen levels are relatively high. Therefore, it should be anticipated that the stainless steel canisters may be coated with carbon steel corrosion products upon removal from the concrete casks.

The consequences of pinhole penetration of the SS canisters has not been considered in detail, but an expected minimal inventory of fission products inside the canisters, combined with slow transport through the pinhole suggests that pinhole penetrations would not result in substantial impacts to the environment inside the concrete casks.

The original work scope requested durability data in the form x±y years. This is most readily accommodated if corrosion data are reported in the format

a±b mil/y. However, this is not the general case, and such data were not available for the cases addressed in the assessment. An alternative approach would be to compare results from different but comparable data sets. However, as indicated earlier, data closely relevant to the relatively benign regimes are largely lacking. Extrapolation from somewhat more aggressive regimes suggests that the results are likely to be conservative, and this is perhaps a more practical and useful perspective than one based on an uncertainty band that has minimal quantitative justification.

7.0 REFERENCES

Bruemmer, S. M., and A. B. Johnson, Jr. 1983. "Effect of Chloride, Thiosulfate, and Fluoride Additions on the IG SCC Resistance of Type 304 Stainless Steel in Low Temperature Water." Proceedings of the International Symposium on Environmental Degradation of Materials in Nuclear Power System-- Water Reactors. Published by National Association of Corrosion Engineers. American Nuclear Society, Myrtle Beach, South Carolina. pp. 571-580.

Craig, B. D. 1991. Fundamental Aspects of Corrosio.. ilms in Corrosion Science. Plenum Press, New York, pp. 115. Note: conclusion regarding pitting also based on discussion with Z. Szklarska-Smialowska.

Johnson, Jr., A. B., and B. Francis. 1980. Durability of Metals from Archaeological Objects, Metal Meteorites, and Native Metals. PNL-3198, Pacific Northwest Laboratory, Richland, Washington.

Kustas, F. M., et al. 1981. Investigation of the Condition of Spent Fuel Pool Components. PNL-3513, Pacific Northwest Laboratory, Richland, Washington.

Robertson, J. 1991. "The Mechanisms of High Temperature Aqueous Corrosion of Stainless Steels." Corr. Sci., Vol. 32, pp. 443-465.

Schmitt, R. C., G. J. Quinn, and M. J. Tyacke. 1993. Historical Summary of the Three Mile Island Unit 2 Core Debris Transportation Campaign. DOE/ID-10400, EG&G, Idaho Falls, Idaho.

Note - References relevant to the corrosion calculations are provided on matrix data sheets in Section 5.0.

DISTRIBUTION

No. of
Copies

OFFSITE

2 DOE/Office of Scientific and
Technical Information

J. Palmer (5)
EG&G Idaho, Inc.
P.O. Box 1625
Idaho Falls, ID 83415-2406

T. McDonald (5)
EG&G Idaho, Inc.
P.O. Box 1625
Idaho Falls, ID 83415-2406

No. of
Copies

ONSITE

DOE Richland Operations Office

G. M. McClure

34 Pacific Northwest Laboratory

A. B. Johnson, Jr. (10)
A. L. Lund (5)
S. P. Pednekar (5)
S. G. Pitman
R. E. Westerman
M. E. Cunningham
R. J. Guenther
E. R. Gilbert
M. D. Freshley
R. E. Einziger
J. L. Ethridge
Publishing Coordination
Technical Report Files (5)